

---

# Contents

|   |     |
|---|-----|
| <b>1 Doppler Sonography: A Brief History</b> .....  | 1   |
| Dev Maulik  |     |
| <b>2 Physical Principles of Doppler Ultrasonography</b> .....   | 11  |
| Dev Maulik  |     |
| <b>3 Spectral Doppler: Basic Principles and Instrumentation</b> .....                                       | 21  |
| Dev Maulik  |     |
| <b>4 Spectral Doppler Sonography: Waveform<br/>Analysis and Hemodynamic Interpretation</b> .....            | 39  |
| Dev Maulik  |     |
| <b>5 Venous Hemodynamics</b> .....  | 63  |
| Torvid Kiserud and Jörg Kessler   |     |
| <b>6 Doppler Color Flow: Basic Principles</b> .....   | 81  |
| Dev Maulik  |     |
| <b>7 Biosafety of Diagnostic Doppler Ultrasound</b> .....   | 99  |
| Kjell Å. Salvesen and Ragnar K. Sande   |     |
| <b>8 Fetal Cardiovascular Physiology</b> .....  | 107 |
| Dino A. Giussani, Kimberley J. Botting, Youguo Niu,<br>Caroline J. Shaw, Sage G. Ford, and Avnesh S. Thakor |     |
| <b>9 Maternal Cardiovascular Physiology and Assessment</b> .....  | 123 |
| Marc E. A. Spaanderman  |     |
| <b>10 Venous Doppler Sonography in Pregnancy</b> .....  | 131 |
| Wilfried Gyselaers  |     |
| <b>11 Relationship Between Maternal and Fetal Cardiovascular<br/>Function</b> .....                         | 145 |
| Christoph C. Lees and Giulia Masini   |     |
| <b>12 Intrauterine Blood Flow and Postnatal Development</b> .....   | 153 |
| David Ley and Karel Maršál  |     |
| <b>13 Fetal Renal Artery</b> .....  | 181 |
| Stephen Contag  |     |

|           |   |     |
|-----------|---|-----|
| <b>14</b> | <b>Umbilical Doppler Velocimetry: Normative Data and Diagnostic Efficacy</b> . . . . .  | 197 |
|           | Dev Maulik, Tabitha Schrufer-Poland, and Emily M. Williams  |     |
| <b>15</b> | <b>Fetal Aortic Isthmus and Descending Aorta</b> . . . . .  | 213 |
|           | Karel Maršál and Edgar Hernandez-Andrade  |     |
| <b>16</b> | <b>The Cerebroplacental Ratio and Hypoxic Index in the Prediction of Fetal Outcome</b> . . . . .  | 243 |
|           | Philippe Arbeille, Gabriel Carles, Gustavo Vilchez, and Dev Maulik  |     |
| <b>17</b> | <b>The Cerebroplacental Ratio</b> . . . . .   | 279 |
|           | Edgar Hernandez Andrade and Eleazar Soto  |     |
| <b>18</b> | <b>Cerebral Blood Flow Velocity Waveforms and Fetal Anemia</b> . . . . .  | 297 |
|           | Jennifer J. Barr and Giancarlo Mari   |     |
| <b>19</b> | <b>First- and Second-Trimester Doppler Velocimetry of the Uteroplacental Circulation</b> . . . . .  | 313 |
|           | Victoria Mumford and Asma Khalil  |     |
| <b>20</b> | <b>Uterine Doppler Velocimetry and Hypertensive Disease</b> . . . . .   | 327 |
|           | Tiziana Frusca, Andrea Dall'Asta, and Elvira Di Pasquo  |     |
| <b>21</b> | <b>Fetal Doppler Velocimetry in Monochorionic Pregnancy: Twin Reversed Arterial Perfusion, Twin-to-Twin Transfusion Syndrome, and Twin Anemia Polycythemia Sequence</b> . . . . . | 337 |
|           | Lee Na Tan, Fionnuala Mone, and Mark D. Kilby   |     |
| <b>22</b> | <b>Doppler Sonography in Pregnancies Complicated by Pre-gestational Diabetes Mellitus</b> . . . . .   | 357 |
|           | Gustavo Vilchez and Dev Maulik  |     |
| <b>23</b> | <b>Doppler Velocimetry in Prolonged Pregnancy</b> . . . . .   | 371 |
|           | Richard Bronsteen, Ali Alhousseini, and Ray Bahado-Singh  |     |
| <b>24</b> | <b>Umbilical Artery Doppler for Fetal Surveillance: Diagnostic Efficacy</b> . . . . .   | 389 |
|           | Dev Maulik and Tara Daming  |     |
| <b>25</b> | <b>Absent End-Diastolic Velocity in the Umbilical Artery and Its Clinical Significance</b> . . . . .  | 399 |
|           | Dev Maulik and Tabitha Schrufer-Poland  |     |
| <b>26</b> | <b>Fetal Doppler Velocimetry in High-Risk Pregnancies: Randomized Clinical Trials</b> . . . . .   | 417 |
|           | Christoph C. Lees and T. Stampalija   |     |
| <b>27</b> | <b>Doppler Interrogation of the Umbilical Venous Flow</b> . . . . .   | 437 |
|           | Enrico Ferrazzi, Daniela Di Martino, and Tamara Stampalija  |     |
| <b>28</b> | <b>The Ductus Venosus</b> . . . . .   | 449 |
|           | Torvid Kiserud and Jörg Kessler   |     |

---

|  |     |
|--|-----|
| <b>29 Doppler Examination of the Fetal Pulmonary Venous Circulation</b> . . . . .                                    | 475 |
| Jay D. Pruetz, Jodie K. Votava-Smith, and Shuo Wang  |     |
| <b>30 Introduction to Fetal Doppler Echocardiography</b> . . . . .   | 499 |
| Dev Maulik and Sarah Hostetter   |     |
| <b>31 Fetal Echocardiography to Plan Postnatal Management in Fetuses with Congenital Heart Disease</b> . . . . .     | 521 |
| Shivani M. Bhatt and Mary T. Donofrio  |     |
| <b>32 Doppler Echocardiography of Fetal Cardiac Arrhythmias</b> . . . . .  | 537 |
| Varsha Thakur and Edgar Jaeggi   |     |
| <b>33 4D Fetal Doppler Echocardiography</b> . . . . .  | 559 |
| Greggory R. DeVore   |     |
| <b>34 Cardiac Function in Fetal Growth Restriction</b> . . . . .   | 575 |
| Giuseppe Rizzo, Ilenia Mappa, Victoria Bitsadze, Jamilya Khizroeva, Alexander Makatsarya, and Domenico Arduini       |     |
| <b>35 Role of Ultrasonography in Placenta Accreta Spectrum</b> . . . . .   | 587 |
| Marcus J. Rijken, Rozi Aditya Aryananda, and Sally Collins   |     |
| <b>36 Three-Dimensional Doppler Ultrasound in Gynecology</b> . . . . .   | 599 |
| Mark Hiraoka and Ivica Zalud   |     |
| <b>37 Doppler Ultrasound in Early Pregnancy Including Miscarriage, Ectopic Pregnancy, and Implantation</b> . . . . . | 615 |
| Mercedes Espada Vaquero, Mathew Leonardi, and George Condous   |     |
| <b>38 Doppler in Benign and Malignant Conditions of the Ovary</b> . . . . .  | 623 |
| Andrea Day and Davor Jurkovic  |     |
| <b>39 Doppler in Benign and Malignant Conditions of the Uterus</b> . . . . .   | 639 |
| Thierry Van den Bosch  |     |

## 5.2 Viscosity Effect on Venous Flow

At high velocity, blood behaves like water, Newtonian, i.e., the viscosity is constant with increasing shear rate. However, when velocities are low, that is no longer the case as viscosity has an increasing effect on the resistance to flow, and energy dissipation, i.e., non-Newtonian.

A clinically important example is the umbilical perfusion of the fetal liver (Fig. 5.6). As much as 70–80% of the umbilical venous return perfuses the liver which has a huge capillary cross section compared with the umbilical vein. Thus, the blood velocity reduces correspondingly when entering the liver parenchyma. With the low velocity, flow is now non-Newtonian and viscous resistance is high. If the perfusion pressure is too low, the blood stops (closing pressure or opening pressure). The viscosity changes with hematocrit, and in particular, the fetal liver perfusion is sensitive to such changes since the driving pressure (umbilicocaval or portocaval pressure gradient) normally operates at a very low level,  $\approx 3$  mmHg [9, 20].

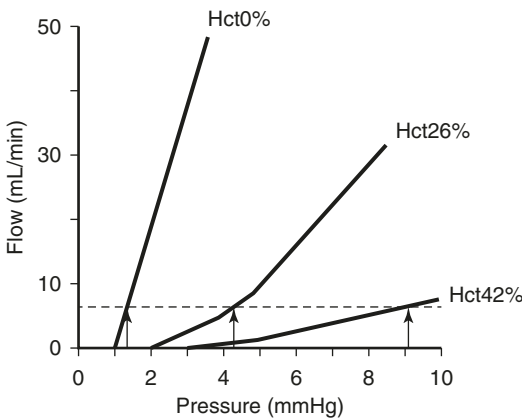


**Fig. 5.6** Effect of blood viscosity on umbilical perfusion of the fetal liver tested in a fetal lamb experiment near term using saline and blood of hematocrit (Hct) 26 or 42% to represent increasing levels of viscosity. Note that the opening pressure (closing pressure) for perfusion is 1, 2, and  $\geq 3.5$  mmHg for Hct 0, 26, or 42%. To maintain a flow of 7 mL/min, a pressure of  $>1$ ,  $>4$ , and  $>9$  mmHg was needed correspondingly (Modified from [21])

This is an important part of the passive regulation of blood distribution between the liver and ductus venosus [21]. Since the ductus venosus has a high blood velocity, it is less affected, and an increase in hematocrit will cause a shift of umbilical blood flow from the liver to the ductus venosus. On top of this comes the active endocrine regulation. Similar effects can be expected in other sections of the circulation where the vascular cross section is large compared with the feeding vessel (e.g., placenta), but the liver portal circuit is special since the feeding vessels are veins with low pressure and velocity compared with circuits fed by arteries.

## 5.3 Pressure Gradient and Resistance in Venous Flow

In any section of the venous system, there is a pressure gradient  $\Delta p$  involved in maintaining a steady flow and overcome resistance ( $R$ ):

$$R = \frac{128\eta L}{\pi D^4}$$

which is dependent on viscosity  $\eta$ , diameter  $D$ , and length  $L$ . There is a long historic discussion whether the ductus venosus has a dedicated muscular sphincter at its inlet to regulate flow (confer Chap. 29). The focus on this short venous section is understandable since the ductus venosus is remarkably narrow, 0.5–2 mm, during the second half of pregnancy [9, 22], and any change in  $D$ , in the power of four, will have a profound effect on  $R$ . However, the isthmus is but a short and ill-defined section of the otherwise long and slender ductus venosus (Fig. 5.7), and experiments have shown that the entire length of the vessel dilates as a response to a hypoxic challenge [23] with a major reduction in  $R$ , which is proportional to  $L$  in the equation. The pressure gradient ( $\Delta p$ ) along the vein, on the other hand, can be calculated as  $\Delta p = R\dot{V}$ , where  $\dot{V}$  signifies blood flow volume, provided the flow is steady without variation in diameter or velocity.

A well-established method of assessing pressure gradients using Doppler ultrasound in

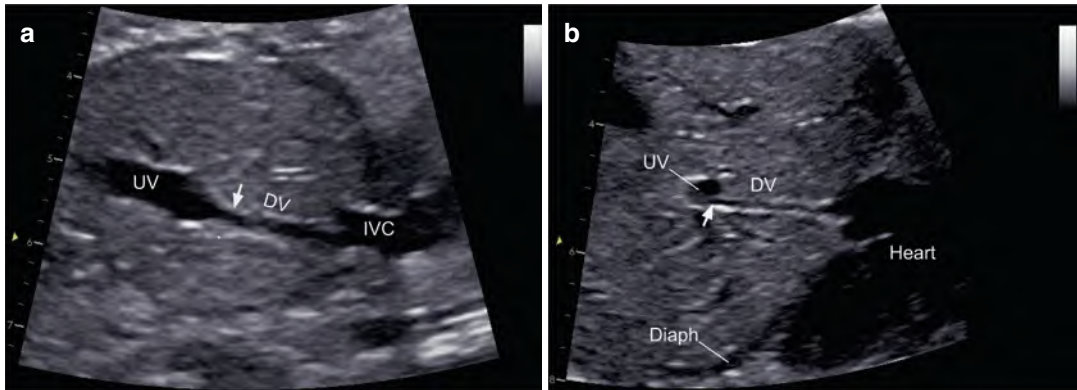


**Fig. 5.7** The shunt ductus venosus (DV) connects the intra-abdominal umbilical vein (UV) to the inferior vena cava (IVC). Typically, it is a slender slightly trumpet-shaped vessel with a narrow isthmus at its entrance (arrow) in panel (a). However, variation in the details is

common such as in panel (b) where almost the entire length of the ductus maintains a similarly small diameter and thus contributes considerably to resistance and flow regulation. *Diaph* Diaphragm

cardiology [24, 25] has also been tested and proven to be valid in the fetal venous system [9, 26]. Since the ductus venosus and the portal circuit in the fetus both connect the intra-abdominal umbilical vein with the IVC, it is possible to exploit the high velocity at the ductus venosus inlet to determine the umbilicocaval (i.e., portocaval)  $\Delta p$ , which is the driving pressure for the venous liver perfusion [9]. Since there is a substantial velocity acceleration as the umbilical blood enters the narrow ductus venosus, the *Bernoulli equation* can be used to calculate  $\Delta p$ :

$$\Delta p = \frac{1}{2} \rho (V_{DV}^2 - V_{UV}^2) + \rho \int_{UV}^{DV} \frac{\delta V}{\delta t} dx + R(V)$$

For practical purposes, this equation can be simplified [9]. The blood density  $\rho$  is  $1.06 \cdot 10^3$ , and in the first term, the umbilical blood velocity  $V_{UV}$  is low compared with the velocity in the ductus venosus  $V_{DV}$ , has little impact on the overall calculation, and is therefore neglected. The second term can be disregarded as it expresses inertia shift and does not impact the magnitude of the  $\Delta p$ . The last term  $R(V)$  represents the viscous resistance and is dependent on the vessel geometry and velocity profile. In the present venous section where blood velocities have some degree of parabolic profile and blood flow has Newtonian

properties, the viscous pressure loss is estimated to be in the order of 0.1 mmHg [26], which is small and therefore also omitted when the simplified version of *Bernoulli equation* is used to determine the pressure gradient:

$$\Delta p = 4V_{\max}^2$$

Here  $V_{\max}$  is maximum blood velocity in m/s at the ductus venosus isthmus and  $\Delta p$  comes directly in mmHg. Further discussion on these issues is available in the literature [9, 24, 25, 27].

Using the simplified *Bernoulli equation*, the umbilicocaval  $\Delta p$  is found to be fairly constant during the second half of pregnancy varying between 0.5 and 3.5 mmHg according to stage of the cardiac cycle if flow is pulsatile (Fig. 5.8). During maximal fetal respiratory activity, pressures up to 25 mmHg can be recorded [9], and the same magnitude is found in the abdominal portion of the IVC [10], both quantifying the capacity of fetal respiratory force.

## 5.4 Measuring Blood Flow in Veins

The volume of blood flow is a fundamental measure in circulation physiology, also in the fetus. Although other noninvasive methods have been used and new are being introduced,

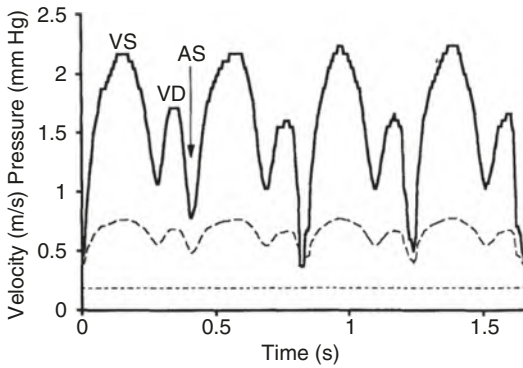


**Fig. 5.8** The umbilicocaval (portocaval) pressure gradient (solid line) in a fetus at 19 weeks' gestation, estimated based on *Bernoulli equation* using Doppler measurements of the ductus venosus blood velocity (broken line) and umbilical venous velocity (dotted line). VS Ventricular systole, VD Ventricular diastole, AS Atrial systole (Modified from [9])

it is the Doppler ultrasound technique combined with biometry of the vessel cross section that provides most of the data available to us today. The technique has been known and used for research purposes for 40 years until it now is increasingly regarded as a possible clinical tool. Two sites have been chosen for the measurement, either the straight portion of the intra-abdominal umbilical vein (preferably distal to the first branching), or a section of the vein in a free-floating loop of the cord [28–35]. Both seem applicable, although the intra-abdominal approach is the more commonly used. Personal skills, optimized equipment and settings, well-founded measurement protocols, and consistency matters when the measurement is made reproducible. Thus, the following paragraphs focus on the key components of blood flow ( $\dot{V}$ ) calculation (usually in mL/min):

$$\dot{V} = \pi \left( \frac{D}{2} \right)^2 h V_{\max} \quad \text{or} \quad \dot{V} = \pi \left( \frac{D}{2} \right)^2 V_{\text{wmean}}$$

i.e., diameter  $D$ , blood velocity  $V_{\max}$  (maximum velocity in the cross section) and  $V_{\text{wmean}}$  (intensity-

weighted mean velocity), and the spatial velocity profile  $h$  (confer Fig. 5.2).

#### 5.4.1 Determining Blood Velocity

In obstetric and fetal medicine environments, too commonly, the quality of the 2D-imaging modalities is prioritized and determines which scanner to be purchased, while assuming that the Doppler functions hold a satisfactory level. However, that is by far not the case. If Doppler recording is priority, it is commendable to have a dedicated machine to crack the toughest Doppler challenges. For most, a sector scanner, rather than a curved or linear transducer, facilitates a perfect alignment of the Doppler beam avoiding the disadvantage of angle correction. As in 2D-imaging, it is an advantage for the Doppler recording to have the option of increasing the ultrasound frequency (MHz), thus refining the resolution of the signal, while reducing the frequency improves the penetration and access to distant vessels.

$V_{\text{wmean}}$  represents the average of all velocities in the sample volume at one point on the timeline of the Doppler recording (Fig. 5.9). The averaged  $V_{\text{wmean}}$  over time is an option for calculating flow. However, this  $V_{\text{wmean}}$  derived from the Doppler shift is easily influenced by signal quality, particularly low-velocity signals such as clutter artifacts along the zero-line, vessel wall movements (Fig. 5.9), loss of low-velocity signals due to filters or inaccurate sample volume placement, interference of neighboring vessels, or loss of weakest signals (i.e., lowest velocities) when recording deep-sited veins. We also have to bear in mind that the Doppler gate (sample volume) is droplet-shaped and hardly ever represents a concise composition of velocities of a vessel cross section. In short, the representation of low velocities from the periphery of the vessel is more likely to be affected and over- or underrepresented in the  $V_{\text{wmean}}$ .

$V_{\max}$ , on the other hand, is merely representing the highest velocity in the vessel cross section (Fig. 5.9). With accurately aligned Doppler insonation and sample volume, this is easily

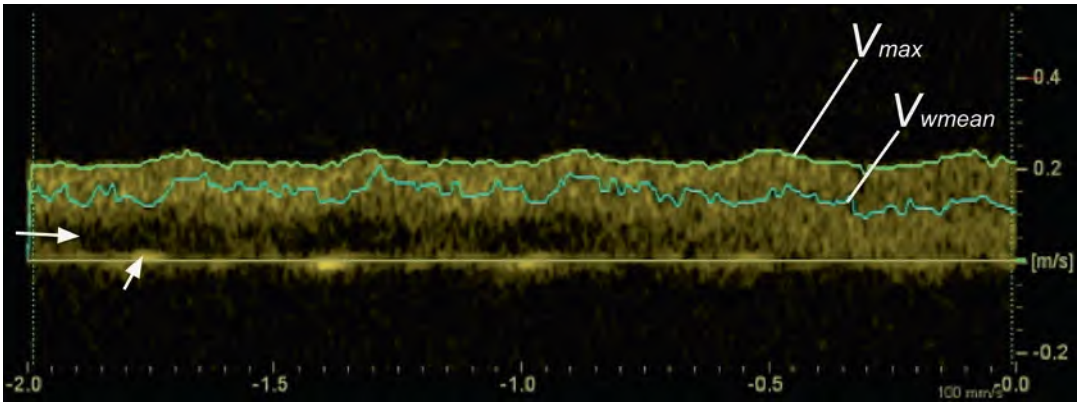


**Fig. 5.9** Doppler recording of the intra-abdominal umbilical vein with automatic tracing of the maximum velocity ( $V_{max}$ ), and, correspondingly, the intensity-weighted mean velocity ( $V_{wmean}$ ). Since  $V_{wmean}$  includes all the velocities recorded, it is susceptible to missing velocity recordings (horizontal arrow), in this case, caused by temporarily dislodged sample volume, leading to an arti-

cially high  $V_{wmean}$  value.  $V_{wmean}$  is also sensitive to wall motion signals along the zero-line (short arrow) correspondingly reducing the  $V_{wmean}$ . Such factors tend to make the  $V_{wmean}$  less reliable than  $V_{max}$ , which, on its side, needs just a sufficiently large sample volume to ensure that the highest velocity is included

recorded, and it constitutes a more robust measurement than  $V_{wmean}$ . However,  $V_{max}$  alone cannot be used in the flow calculation without including the constant  $h$  for the spatial velocity profile. In the sections of intra-abdominal umbilical vein where the flow is steady, it should be parabolic and correspondingly  $h = 0.5$ , which is supported by studies [34, 36]. However, for the umbilical venous flow at the placental cord insertion with accelerating velocities,  $h$  will be higher, and even more so at the physiological vein constriction at the abdominal wall. Similarly, in the ductus venosus entrance, the blunted profile of  $h = 0.7$  is well-documented [11, 14].

Which method should be preferred for venous flow calculation? The literature has examples of both alternative flow calculations [22, 28, 29, 31, 32, 37–39]. For sections that have been more thoroughly explored (e.g., ductus venosus and intra-abdominal umbilical vein), it is probably safer to use the experimentally validated method of maximum tracing of the Doppler velocity recording combined with the corresponding velocity profile  $h = 0.7$  and  $0.5$ . However, in first trimester when velocities are generally lower, the ductus venosus flow has  $h = 0.53$ , i.e., practically parabolic [40]. Such standardization makes the volume flow assessment less prone to technical

errors and artifacts due to interference from neighboring vessels, wall motion, and low-velocity artifacts.

## 5.4.2 Determining Vessel Diameter

When calculating blood flow, diameter measurement stands out as a contributor to random error because it is magnified by the power of two in the equation, and the smaller the diameter, the higher the relative risk of error will be [41, 42]. So, there is good reason to search all possibilities to control such errors.

First, choice of equipment makes a difference: high frequency transducer rather than lower frequency, a linear scanner focuses better than others, single frequency is commonly an advantage to harmonics, and a standardized set up reduces random error.

The site of measurement should be where the Doppler was recorded, but perpendicular to the vessel wall as that gives the best definition of the interface between vessel wall and blood. Measurements in a lateral direction to the ultrasound beam should preferably be avoided as the interfaces are less well-defined, the resolution inferior, and prone to overestimation.

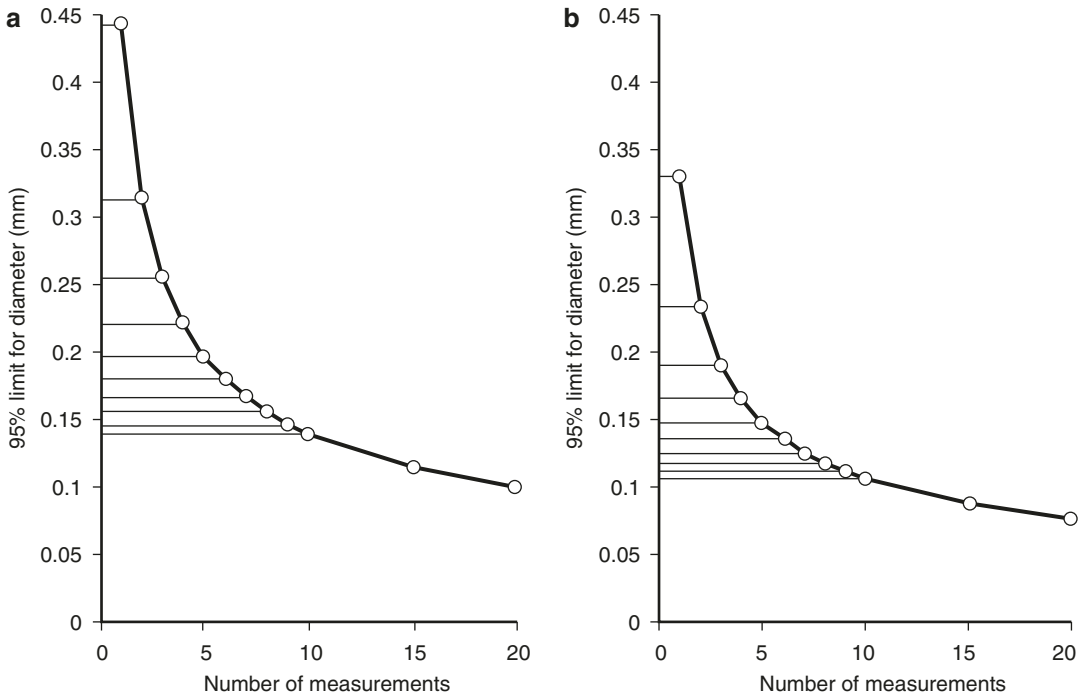


**Fig. 5.10** Repeat measurement of diameter is a powerful method of reducing random error of the vessel cross section, here exemplified by the intra-abdominal umbilical

vein (a) and ductus venosus (b) and presented with the upper 95% CI limit for variation. (Modified from [41])

Early works commonly used the leading-edge principle, that is outer-inner measurement since that ensured consistency with the technology of the day [43]. That explains some of the variance compared with modern studies using the inner-inner measurement technique, the presently preferred method [41].

Repeat measurement is a commendable and powerful method of reducing random error (Fig. 5.10), which is important particularly in small bore vessels such as the ductus venosus [41, 42]. E.g., with an umbilical vein diameter of 4 mm, the 95% IC for blood flow estimation reduces from  $\pm 23\%$  to  $\pm 13$  or  $\pm 9\%$  if the diameter is based on 3 or 6 measurements, respectively. On the other hand, for the slim ductus venosus with a diameter of, e.g., 1.5 mm, the flow error reduces from  $\pm 49\%$  to  $\pm 27$  or  $\pm 18\%$  when the diameter measurement is repeated 3 or 6 times, respectively. And, further improvement is achieved when repeating 10 or 20 times, yielding

$\pm 13$  or  $\pm 10\%$  error (for the ductus). Yet, as both numbers and graphs indicate (Fig. 5.10.), the benefit tapers off with increasing number of measurements and time consumed.

Semiautomated diameter measurement has been suggested and used (Fig. 5.11.) [44, 45]. The method is originally designed for standardized measurement of fetal nuchal translucency. When applied in measuring umbilical vein diameter, it was shown to reduce intra- and interobserver variation, thus being relevant candidate for vessel measurement protocols.

## 5.5 Pulsation in Veins

The blood velocity pulse recorded with our Doppler equipment is just one part of the entire pulse, the other components being a pressure wave and a diameter wave, together following the principle of energy preservation for motion of



**Fig. 5.11** Semiautomated diameter measurement of the umbilical vein (here at 12 weeks' gestation) is a suggested method of reducing intra- and interobserver variation. (Modified from [44])

incompressible fluids as described in Navier-Stokes' equations [1]. Here, we highlight some consequences that may help us interpret our recordings.

### 5.5.1 Transmission Lines

The pulse generated in the heart is not transmitted equally well in all tissues. It travels better along transmission lines, and arteries and veins connected to the heart constitute such transmission lines. While blood flow velocity in the venous system rarely exceeds 1 m/s, the pulse wave travels faster, typically 1–2.5 m/s in the umbilical vein [46]. The stiffer the vessel wall is, the faster it runs. An important transmission line is formed by the IVC, ductus venosus, and umbilical vein (Fig. 5.12) [47, 48]. Agenesis of the ductus venosus has been shown to interrupt the transmission of the cardiac wave to the umbilical vein [12]. The wave propagating along this line reflects the changes in both the left and the right atrium since the IVC is connected to the left atrium through the foramen ovale in addition to the connection to the right atrium. Conversely, the pulmonary veins reflect predominantly the left atrium, and to some extent the right atrium, depending on the size of the foramen ovale [49].

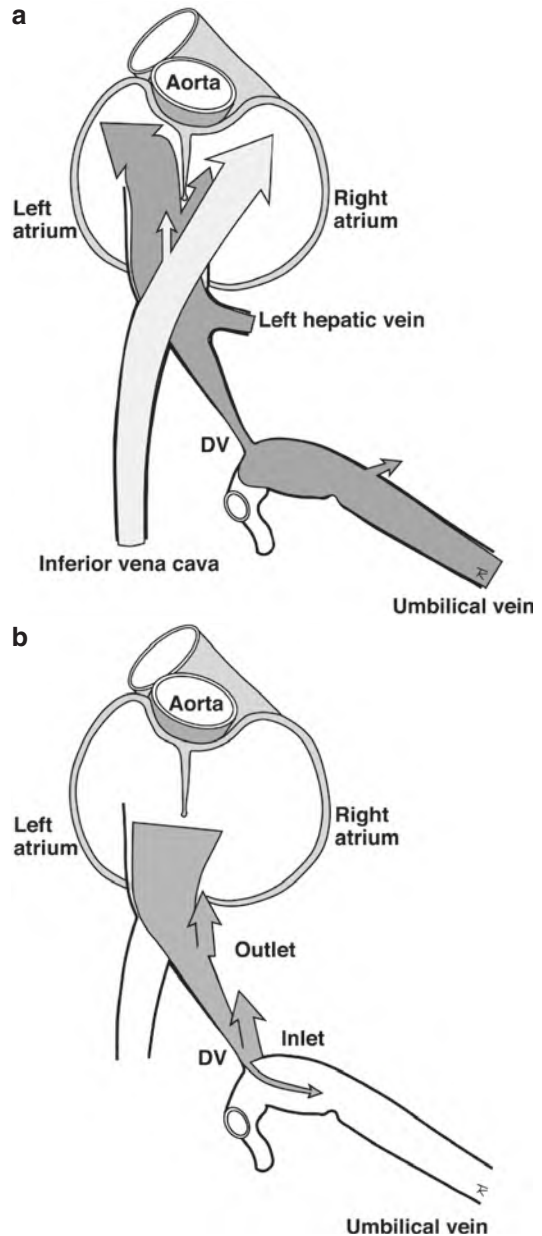


**Fig. 5.12** The same veins that direct blood toward the heart (a) act as transmission lines in the opposite direction for pulse waves generated in the heart. The most studied transmission line is formed by the proximal portion of the inferior vena cava, ductus venosus (DV), and the umbilical vein (b). The wave is partially reflected at the junctions according to the difference in impedance above and below the junction (broad arrows). Due to the large difference in impedance between the ductus venosus inlet and the intra-abdominal umbilical vein, most of the wave is reflected at this junction. The small wave energy (slim arrow) transmitted into the umbilical vein is usually not enough to cause visible velocity pulsation at this site. (Modified from [48, 50])

### 5.5.2 Wave Reflections

The pulse wave traveling along the transmission line is modified according to the local physical conditions [1, 13, 14, 16, 26, 47, 49, 51]. Pulsation at the ductus venosus outlet is more pronounced than at the inlet [52]. The stiffness of the vessel wall is different at the ductus venosus outlet, ductus venosus inlet, and intra-abdominal umbilical vein, and so are cross section and compliance [46]. The single most important mechanism for changing the propagating pulse in the veins is reflections. In much the same fashion as light is reflected or transmitted when the beam encounters a medium with a different density, the pulse wave in the veins is reflected and transmitted when it hits a change in impedance (Fig. 5.12b) [47, 48, 53]. Vascular junctions often represent a significant change in cross section (and thus impedance). The junction between the ductus venosus inlet and the umbilical vein is of great diagnostic interest and has been particularly well-examined. During the second half of pregnancy, pulsation is regularly observed at the ductus venosus inlet, but on the other side of the junction, millimeters away, there is no pulsation in the umbilical vein velocity. The reason is reflections [53]. The Reflex coefficient ( $R_c$ ) determines the degree of reflection and depends on the impedance of the two sections of veins (e.g.,  $Z_{DV}$ , ductus venosus, and  $Z_{UV}$ , umbilical vein):

$$R_c = \frac{\text{Reflected wave}}{\text{Incident wave}} = \frac{Z_{UV} - Z_{DV}}{Z_{UV} + Z_{DV}}$$

In this case,  $Z_{UV}$  represents the terminal (distal) impedance in fluid-dynamic terms, whereas  $Z_{DV}$  represents the characteristic impedance. From a practical point of view, the single most important determinant for impedance is the cross section of the vessel (A):

$$Z = \rho c / A$$

( $\rho$  = density, and  $c$  = wave velocity). In the case of the ductus venosus–umbilical vein junction, there is an extraordinary difference in cross section, and thus impedance; the ratio of the diameter of the umbilical vein and the ductus venosus

being 4 (95% CI 2; 6) [47]. Correspondingly, most of the wave will be reflected and little energy transmitted further down. The small proportion of the energy transmitted to the umbilical vein, commonly, is not sufficient to cause visible pulsation. In extreme conditions, such as during hypoxia, the ductus venosus distends [23, 54], and the difference in vessel area between the two sections is reduced, and less wave is reflected and more transmitted (Fig. 5.13a); thus, a larger proportion of the wave arrives in the umbilical vein and may induce pulsation, particularly if the a-wave was augmented in the first place.

In 3% of all recordings, there is no pulsation in the ductus venosus (Fig. 5.14a), which is a normal phenomenon [55]. The pattern is in many cases caused by the position of the fetus bending forward and thus squeezing the IVC and ductus venosus outlet (Figs. 5.13b) [47]. The extensively reduced cross section causes a total reflection of wave at the level of the IVC–ductus venosus junction and hardly any pulse is transmitted further down until the squeeze has been released (Fig. 5.14b). A similar effect can probably be obtained by the spontaneous variation in cross section sometimes seen in the proximal portion of the IVC.

### 5.5.3 Direction of Pulse and Blood Velocity

We are well-acquainted with blood pressure wave traveling down our brachial artery associated with corresponding transient rise in blood velocity, the velocity pulse. On the venous side, however, this is inversely related; the pressure pulse from the heart travels down the venous system but causes a velocity deflection, the reason being that the pressure this time is imposed on flow in the opposite direction, toward the heart (Fig. 5.15 upper panel). The phenomenon is addressed in the concept of “wave intensity” introduced to explain the wave in arteries [56], but the concept is equally valid for veins [49, 57].

A particularly instructive example is found in the left portal branch (Fig. 5.15 lower panel), where the negative velocity wave of the umbilical

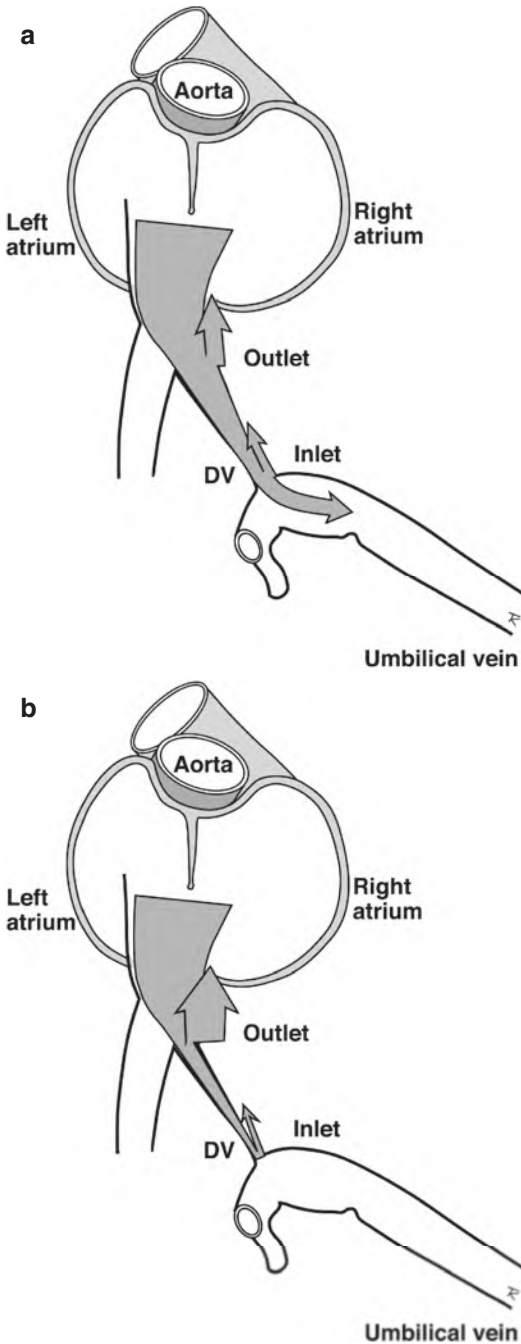


**Fig. 5.13** A distension of the ductus venosus (DV) inlet and increased tone in the umbilical vein with reduced diameter reduce the difference of impedance between the two sections. Correspondingly, less reflection and more transmission increase the likelihood that velocity pulsations are observed in the umbilical vein (a). When the DV is squeezed right up to the outlet, a larger proportion of the wave is reflected at the level of outlet (b), leaving little wave energy to be transmitted further down the transmission line. No pulsation may then be observed at the DV inlet. (Modified from [48])

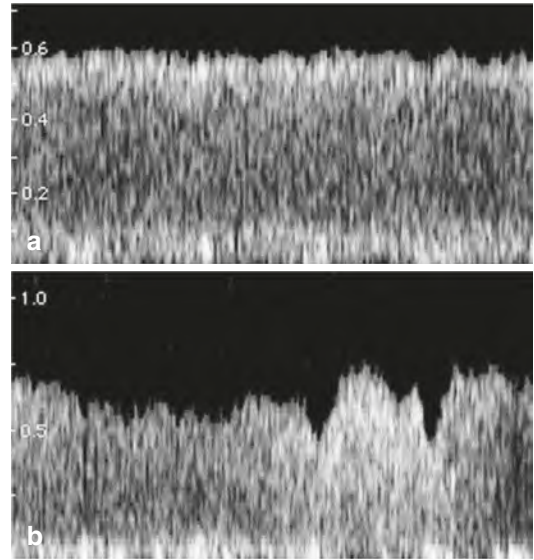


**Fig. 5.14** Doppler recording of the ductus venosus blood velocity without pulsation (upper panel) due to the fetal position bending forward and squeezing the ductus venosus outlet. The wave has been completely reflected at the junction with the inferior vena cava (see Fig. 5.13b). Seconds later, a change in fetal position restores the dimension of the vessel (corresponds to Fig. 5.13a) and the pulsatile flow pattern (lower panel). (Modified from [48])

vein (Fig. 5.15 upper panel) has turned positive [57]. The explanation is as follows. Blood flows up the umbilical vein toward the ductus venosus and heart, but is also directed into the left portal branch (the transverse sinus (Fig. 5.16)). The pressure wave from the heart is traveling in opposite direction and imposes a negative atrial contraction wave in the ductus venosus and umbilical vein. This pressure wave, however, also propagates into the left portal branch now running in the same direction as the blood flow there and, accordingly, the atrial contraction wave turns positive (Fig. 5.15 lower panel).

In the compromised fetal circulation, the left portal vein also acts as a watershed area between the left and right part of the liver [57–59]; thus, blood velocity in this section may be low, pendulate, or reversed. Depending on the direction of flow in this section, the waveform will turn the same way or be inverted when compared with the umbilical vein pulse.

This effect of mirroring waves is particularly observed when the wave is augmented as in placental compromise causing cardiac decompensation.

**Fig. 5.15** *Upper panel:* When the pressure pulse and blood velocity travel in *opposite* directions, the resulting velocity change during the pulse will be a deflection. A common example is the atrial contraction wave recorded in the umbilical vein (A). *Lower panel:* When the pressure pulse and blood flow travel in the *same* direction, the resulting blood velocity change during the pulse will be an increase. Accordingly, the atrial contraction wave recorded in the left portal vein is recognized as a peak (A). For further explanation see Fig. 5.16. (Modified from [57])

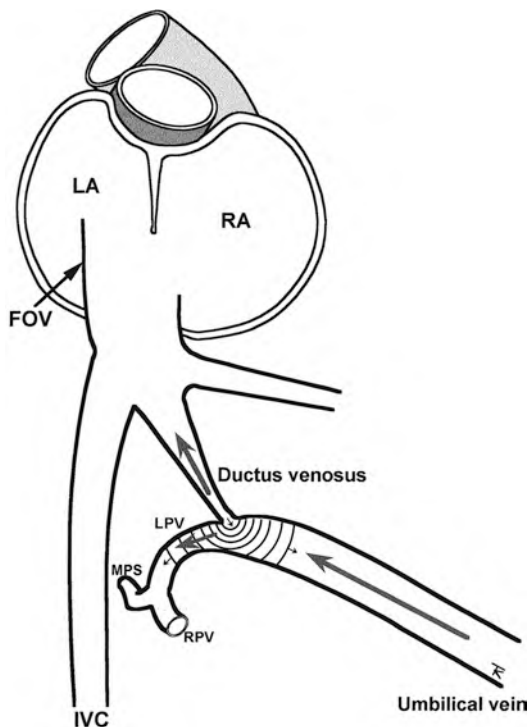
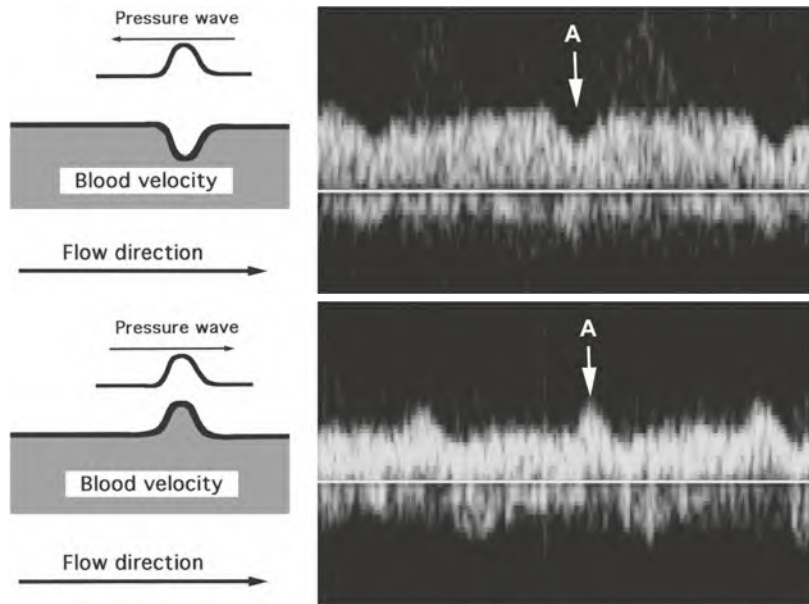


**Fig. 5.16** The pressure pulse emitted from the heart travels along the veins acting as transmission lines. When the pulse reaches the junction between the ductus venosus inlet and the umbilical vein, the pulse wave (concentric rings and minute arrows) continues in two directions: (1) along the umbilical vein *against* the flow direction (large arrows), or (2) follows the left portal branch (LPV) into the liver *with* the flow direction. FOV Foramen ovale valve, IVC Inferior vena cava, LA Left atrium, MPS Main portal stem, RA Right atrium, RPV Right portal branch. (Modified from [57])

The same wave with an augmented amplitude found at the ductus venosus isthmus is imposed on the left portal vein, but inverted (Fig. 5.17). Although essentially being the same pressure wave imposed on the two different venous sections, the calculated pulsatility in the left portal vein comes out substantially higher than for the ductus venosus. The reason is that the time-averaged velocity (included as denominator in the index) is much lower in the left portal vein than in the ductus venosus.

#### 5.5.4 Compliance and Reservoir Function of the Umbilical Vein

Another determinant affecting pulsation is the reservoir effect [51]. Whether a pulse that arrives in the umbilical vein induces velocity pulsation depends on the amount of energy it carries and the local compliance. The umbilical vein is a sizeable vessel and acts as a reservoir. The larger and more compliant the reservoir is, the higher wave energy is required to induce a visible pulsation of the blood velocity (Fig. 5.18). Accordingly, pulsation should be a rare event in late pregnancy, whereas the small vascular dimensions in early pregnancy predispose for pulsation. Correspondingly, pulsation in the umbilical vein is reported as a normal phenomenon, particularly before 13 weeks of gestation [60]. It follows that an increased tone of the

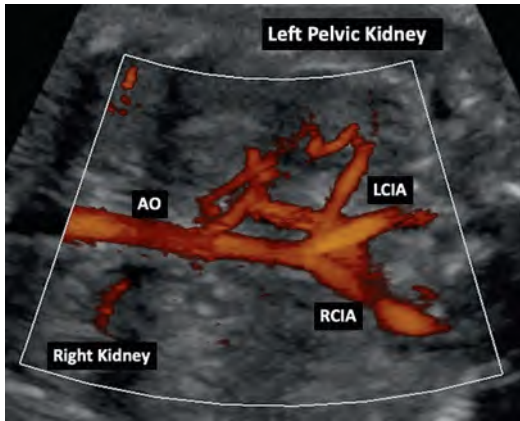


**Fig. 6.15** Power Doppler image of renal vascular supply of a fetal pelvic kidney. The Doppler image is confirmatory of B-mode finding. Note monochromatic color flow with no demonstrable angle effect. *AO* Aorta, *RCIA* Right common iliac artery, *LCIA* Left common iliac artery

The amplitude output is affected by the wall (high-pass) filter as it removes high-amplitude/low-frequency Doppler signals generated by tissue movements. If the filter setting were identical to the frequency-based color flow mapping, the amplitude map would offer no more flow information than the former. Current filter algorithms, particularly those utilizing the multivariate approach, have substantially minimized this problem. An appropriate filter setting is essential for optimal color Doppler amplitude imaging. A low threshold of wall filter is needed for identifying low-flow states. Doppler power, or energy, imaging is also affected by the gain (Fig. 6.16). A high gain results in increased sensitivity for detecting slow-velocity circulations, but also in blooming artifacts where color flow areas extend beyond the vascular margin overwriting B-mode tissue signals. Other factors that interdependently or independently affect the power or energy mode display include the transmitted acoustic power, depth, color sensitivity, preponderance of gray scale (write priority), and persistence. The implementation of these controls and the resultant changes in the amplitude color maps vary from device to device. Most devices offer application specific default settings.

Over the recent years, significant technological advances have substantially expanded the

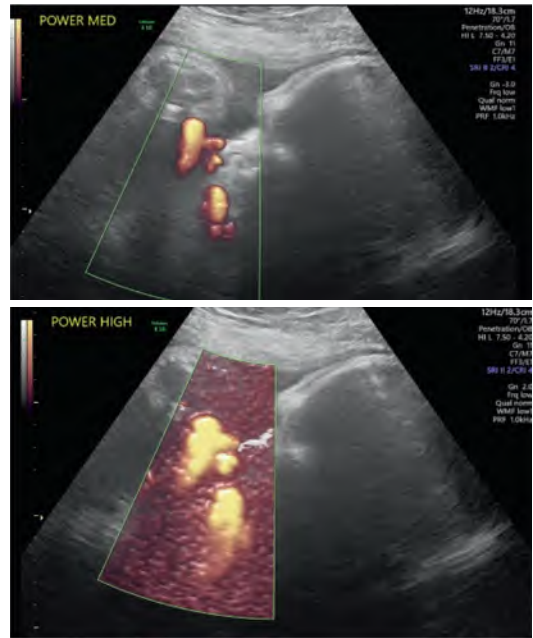


**Fig. 6.16** Power Doppler images of umbilical artery demonstrating the effect of increasing the gain from medium (upper panel) to high (lower panel)

capabilities of the power Doppler imaging and enhanced its clinical utility. These include directional power Doppler and power Doppler microvascular imaging and are presented below.

### 6.6.1 Directional Power Doppler

One of the advances in power Doppler imaging is the incorporation of directional information from the Doppler frequency shift signals into the Doppler power or amplitude signals, thus expanding its hemodynamic information content. In high definition power Doppler, short pulses with smaller Doppler sample volumes are used to obtain the flow direction. The advantages include improved axial resolution, lessening of blooming artifacts, better adaptive filtering of clutter signals, and higher temporal resolution. Preliminary reports demonstrated the potential of this modality in assessing fetal heart, prenatal diagnosis of cleft lip, and adult hepatic circulation [6–8]. The superior flow imaging capability of directional power Doppler compared to color Doppler and

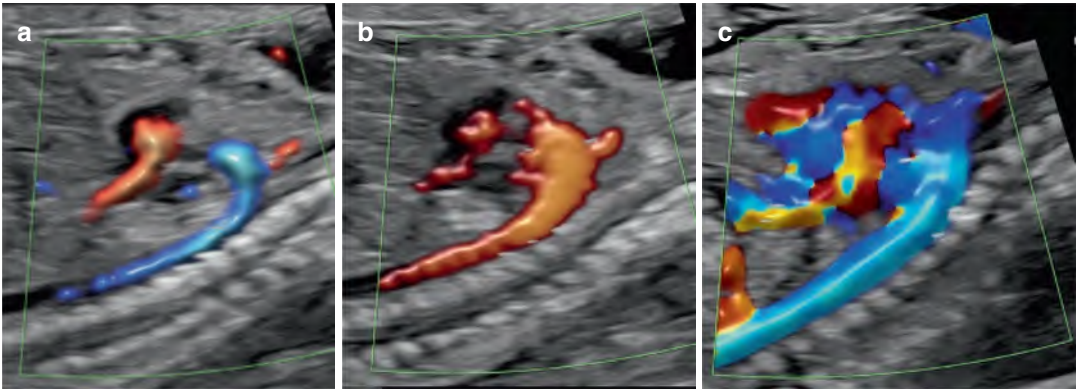


**Fig. 6.17** Comparison of color Doppler (A), power Doppler (B), and directional power Doppler (C) images of fetal aortic flow

nondirectional power is illustrated in Fig. 6.17. The directional power Doppler image showed clearly defined flow through the whole length of the aorta within the color window without any loss of signal from the angle effect. Photorealistic visualization technique as described above was used in all three Doppler images, providing a simulated 3D appearance with clearly defined vascular margins (Radiantflow™, GE).

### 6.6.2 Power Doppler Microvascular Flow Imaging

In microvascular flow imaging (MVFI), advanced adaptive filtering techniques have been developed to eliminate high-amplitude low-frequency clutter signals from the low flow low-amplitude signals from small vessels. This approach results in exceptional sensitivity and spatial resolution in microvascular imaging. Preliminary experience has demonstrated its superiority over color Doppler and power Doppler imaging for assessing thyroid microvascular circulation in normal thyroid tissue and thyroid nodules [9]. More recently, MVFI has shown a significantly greater sensitivity and accuracy in detecting intratumor vascularity in hepatocellular tumor compared to color or power Doppler [10]. Our own initial imaging experience shows its potential for investigating fetal microcirculation in organs such as



**Fig. 6.18** Microvascular power Doppler imaging of fetal hepatic circulation

the fetal liver (Fig. 6.18). Noteworthy is the spatial resolution of the small vasculature (MV-Flow™, Samsung), further enhanced by 3D visualization as discussed earlier ((Lumiflow™, Samsung).

## 6.7 Four-Dimensional Doppler Color Flow Mapping

Color Doppler has also been implemented in four-dimensional (4D) imaging and has been applied in fetal hemodynamic assessment.

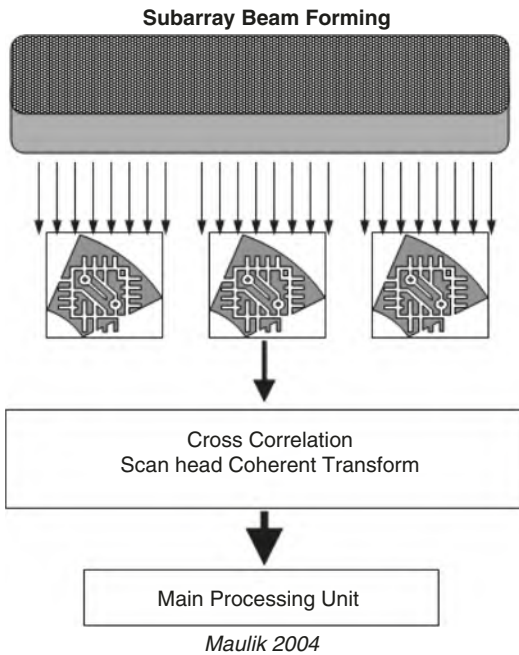


**Fig. 6.19** Graphic depiction of the concept of sub-array beam forming

Initially, this was implemented with a motor driven mechanical probe, which generates a reconstructed 3D image volume. Significant advances have occurred in this field with the innovation of matrix array technology which allows electronic 3D volume generation in real time. The two-dimensional matrix array transducers utilize thousands of piezoelectric elements, all of which transmit and receive ultrasound. The enormous volume of data thus generated are processed in real time by sub-array beamforming involving several custom integrated circuits located in the handle of the transducer, and then transmitted to the main computer system of the device for further processing and generation of 3D images in real time (Fig. 6.19). The inherent limitations of Doppler sonography such as angle dependence are valid in these modalities.

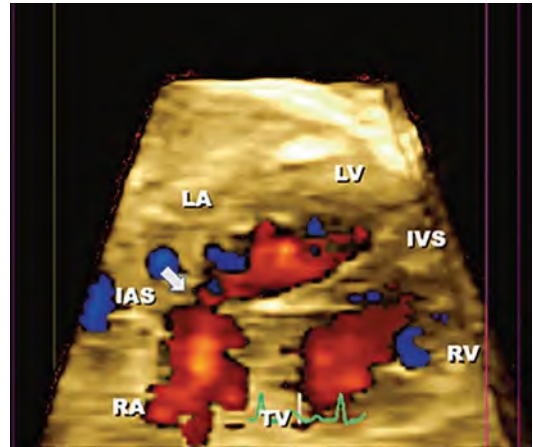


**Fig. 6.20** Four-dimensional echocardiography using a two-dimensional matrix phased array in a fetus depicting interatrial flow. Arrow points to the foramen ovale. RA Right atrium, LA Left atrium, RV Right ventricle, LV Left ventricle, TV Tricuspid valve, IVS Interventricular septum, IAS Interatrial septum

It was initially introduced as a phased array system and shown to be effective in demonstrating normal and abnormal fetal cardiac anatomy and flow dynamics (Figs. 6.20 and 6.21) [11]. More recently, curved array matrix technology has been introduced and applied for fetal echocardiography [12].

The unit of three-dimensional spatial graphic information is known as a voxel, which can be digitally quantified to represent objective properties such as opacity, density, color, velocity, or even time. The ability to modify the opacity of a voxel is critical for three-dimensional imaging. This is known as opacity transformation which allows visualization of internal morphology of an image which would otherwise be obscured by more opaque surface voxels. An example of transparency mode (glass body) depiction of aortic and pulmonary cross-over view is given in Fig. 6.22. A review of the 4D Doppler echocardiography is presented in Chap. 33.

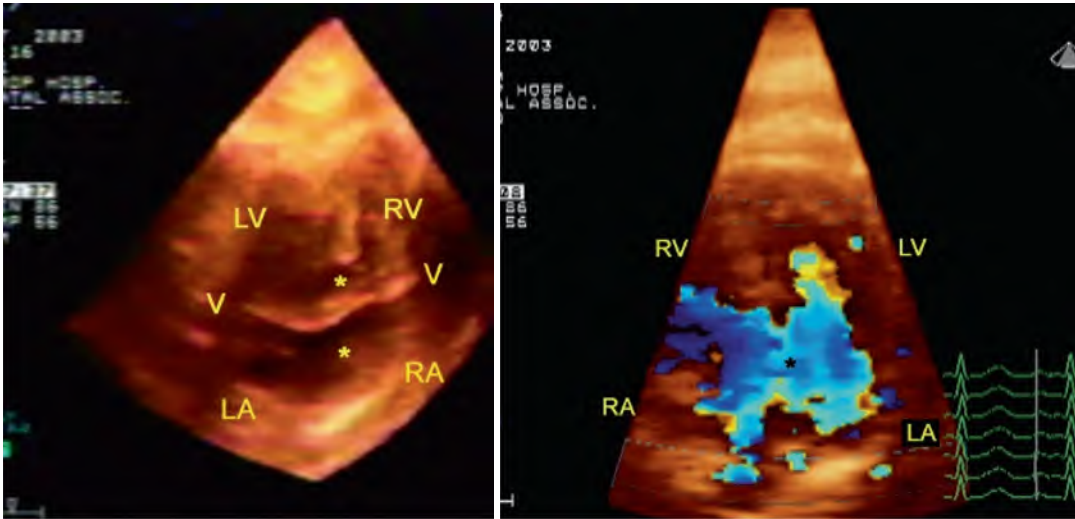


**Fig. 6.21** Four-dimensional echocardiography using a two-dimensional matrix phased array in a fetus with complete atrioventricular septal defect. Four-chamber view cropped to show the atrial and ventricular septal defect with common atrioventricular valve (left panel) and color

Doppler depiction of shunt across the septal defect (right panel). RA Right atrium, LA Left atrium, RV Right ventricle, LV Left ventricle, V Common atrioventricular valve. (With permission from reference [12])

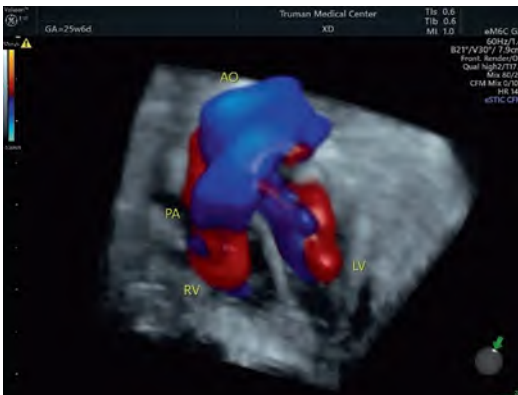


**Fig. 6.22** Four-dimensional echocardiography of the aortic and pulmonary cross-over relationship using a two-dimensional matrix curved array transducer, and Radiantflow™ with transparency or glass body mode. AO Aorta, PA Pulmonary artery, LV Left ventricle, RV Right ventricle

## References

1. Omoto R, Kasai C. Physics and instrumentation of Doppler color flow mapping. *Echocardiography*. 1987;4:467–83.
2. Lee R. Physical principles of flow mapping in cardiology. In: Nanda NC, editor. *Textbook of color Doppler echocardiography*. Philadelphia: Lea & Febiger; 1989. p. 18.
3. Kremkau FK. Principles of color flow imaging. *J Vasc Tech*. 1991;15:104–9.
4. Namekawa K, Kasai C, Tsukamoto M, Koyano A. Real time bloodflow imaging system utilizing auto-correlation techniques. In: Lerski R, Morley P, editors. *Ultrasound "82"*. London: Pergamon; 1983. p. 203–8.
5. Angelsen BAJ, Kristoffersen K. On ultrasonic MTI measurement of velocity profiles in blood flow. *IEEE Trans Biomed Eng*. 1979;26:665–71.
6. Hata T. Modern 3D/4D sonographic studies on fetal heart. *Ultrasound Rev Obstet Gynecol*. 2006;6:115–22.
7. Kennelly MM, Moran P. Directional power Doppler in the midsagittal plane as an aid to the prenatal diagnosis of cleft lip and palate. *Prenat Diagn*. 2008;28(1):56–8.
8. Kim SH, Lee JM, Kim YJ, Lee JY, Han JK, Choi BI. High-definition flow Doppler ultrasonographic technique to assess hepatic vasculature compared with color or power Doppler ultrasonography: preliminary experience. *J Ultrasound Med*. 2008;27:1491–501.
9. Machado P, Segal S, Lyshchik A, Forsberg F. A novel microvascular flow technique: initial results in thyroids. *Ultrasound Q*. 2016;32:67–74.
10. Kang HJ, Lee JM, Jeon SK, Ryu H, Yoo J, Lee JK, Han JK. Microvascular flow imaging of residual or recurrent hepatocellular carcinoma after transarterial chemoembolization: comparison with color/power doppler imaging. *Korean J Radiol*. 2019;20:1114–23.
11. Maulik D, Nanda NC, Singh V, Dod H, Vengala S, Sinha A, Sidhu MS, Khanna D, Lysikiewicz A, Sicuranza G, Modh N. Live three-dimensional echocardiography of the human fetus. *Echocardiography*. 2003;20:715–21.
12. DeVore GR, Satou G, Sklansky M. 4D fetal echocardiography—an update. *Echocardiography*. 2017;34:1788–98.



# Biosafety of Diagnostic Doppler Ultrasound

# 7

Kjell Å. Salvesen and Ragnar K. Sande

## 7.1 Introduction

Ultrasound has an enviable safety record. Despite its use for almost 50 years, there are no proven harmful effects in humans. It would be wrong, however, to suppose that this risk does not exist. Ultrasound is used for tissue ablation and surgery, to lyse cells and create emulsions, to melt metal, and has been investigated for use as a weapon.

There are two major concerns; the vast number of babies exposed during fetal life, and gaps in knowledge about ultrasound safety. Most developed countries offer from one to four routine ultrasound examinations to all pregnant women. Many of these are carried out using new generations of ultrasound scanners, which have the potential to produce higher acoustic outputs than older devices. Furthermore, there are many gaps in our knowledge about ultrasound safety. Many of the studies on which we base our recommendations have been carried out in animal mod-

els whose relevance to the human is poorly understood, ultrasound exposure conditions which have little relevance to diagnostic ultrasound pulses, or on scanners that are no longer in common clinical use.

When reading this chapter, it must be remembered that absence of evidence of harm is not the same as absence of harm. It is never possible to prove a negative (“there is no such thing as zero risk”). It should also be remembered that Doppler ultrasound always has the highest risk of producing adverse effects, and that there are hardly any human data regarding safety of Doppler ultrasound.

## 7.2 Acoustic Output from Diagnostic Scanners

The lack of a consistent method of describing “dose” has made interpreting studies of ultrasound bioeffects difficult. Ultrasound fields are described in terms of pressure or intensity, neither of which give a measure of energy deposition. Nevertheless, acoustic power and intensity are of central importance when considering their safe use.

Acoustic power is a measurement of the rate at which the energy is emitted by the transducer measured in watts (joules per second). Acoustic powers in diagnostic beams vary from less than 1 mW to several hundred milliwatts. All this power is absorbed by the tissue, and the temperature can be raised.

---

K. Å. Salvesen (✉)

National Center for Fetal Medicine, Department of Obstetrics and Gynecology, St. Olavs Hospital, Trondheim University Hospital, Trondheim, Norway

Institute of Clinical and Molecular Medicine, Norwegian University of Science and Technology (NTNU), Trondheim, Norway  
e-mail: [pepes@ntnu.no](mailto:pepes@ntnu.no)

R. K. Sande

Department of Obstetrics and Gynecology, Stavanger University Hospital, Stavanger, Norway

It is also relevant to describe how the power is distributed throughout the beam and across the scanning plane. This variation is measured as acoustic intensity, which is obtained by averaging the power over an area. The practical unit of measurement is milliwatt per square centimeter ( $\text{mW}/\text{cm}^2$ ). A commonly quoted intensity is the spatial-peak temporal-average (SPTA), which is the greatest intensity in the beam (where the beam is “brightest”). For pulsed Doppler, this will be in the focal zone.

Modern ultrasound scanners have become so complex and have so many different output combinations that it is impossible for anyone other than the manufacturer or a specialized laboratory to measure the output. The most comprehensive surveys of acoustic output values for ultrasound systems were published in the 1990s [1–3], and one survey was published in 2010 [4] (Fig. 7.1).

This figure demonstrates that the most recent survey (2010) found an increase for B-mode (green bars), but a reduction for pulsed Doppler mode (red bars) compared to 1998 values, result-

ing in increased overlap in values between modes. But the figure also shows that maximum values are more than 1000 times greater than those reported for the first real-time B-mode scanners, and that the highest values are for pulsed Doppler ultrasound.

### 7.3 Safety Standards and Regulation

Pressure, intensity, and power parameters describe the acoustic field and are related to the field the patient is exposed to during diagnosis. However, they are not good indicators of the risk of adverse effects. Current standards and regulations refer to parameters intended to relate more directly to cavitation (bubble formation) and tissue heating (temperature rise). The mechanical index (MI) indicates the probability of cavitation, and the thermal index (TI) is an indicator of the likely maximum temperature rise in tissues exposed to ultrasound.

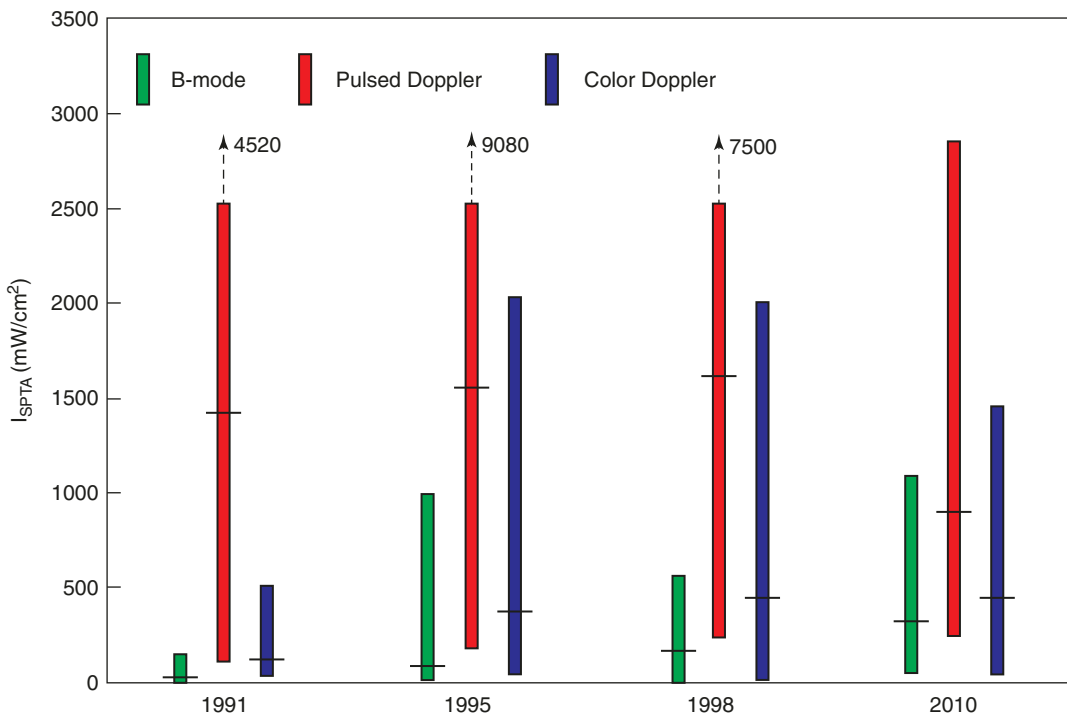


**Fig. 7.1** Manufacturer declared values of spatial-peak temporal-average (SPTA) intensity from surveys in 1998–2010 in B-mode, pulsed Doppler, and color Doppler mode (Modified from Martin 2010 [4])

In 1991, the maximally permitted intensity during obstetric scanning was increased from 94 mW/cm<sup>2</sup> to 720 mW/cm<sup>2</sup> [5]. In order to maintain the safety of obstetric scanning, all scanners able to produce intensities above 94 mW/cm<sup>2</sup> were required to display TI and MI on-screen during the examination. The examiner is responsible for the safety of the examination; the TI and MI are meant to be an aid to the examiner in making sure that the ultrasound exposure is limited to what is needed to obtain the necessary clinical information [6].

---

## 7.4 Thermal Index

The formula for the TI is as follows:

$$TI = W_0 / W_{1c}$$

$W_0$  is the power currently being used, and  $W_{1c}$  is the power needed to raise the tissue temperature by one degree Celcius, in a reasonable worst-case scenario steady state. It thus follows that a TI of 1.0 corresponds to a maximal theoretical increase in tissue temperature of 1.0 degrees Celcius; a TI of 2.0 corresponds to a maximal theoretical increase in tissue temperature of 2.0 degrees Celcius, etc.

Different tissues have different ultrasound absorption properties, therefore three different versions of the TI have been developed; the TI for soft tissue (TIS), to be used when there is only soft tissue in the scanning field, TI for bone (TIB) to be used when there is bone present in the field, and TI for cranial bone (TIC) for direct cranial insonation. The British medical ultrasound society (BMUS) recommends the use of TIB from week 10 of pregnancy [7].

The TI is a rough estimate for exposure, based on power, modality, and scanning depth, as such it can never be 100% accurate. It has been criticized for being too inaccurate to be of clinical use, due to an unclear definition and calculation difficulties [8]. Considerable inconsistency has been found between TIB and the corresponding measured intensities in vitro [9].

## 7.5 Mechanical Index

The formula for the MI is as follows:

$$MI = PNP / \sqrt{F_c}$$

PNP is the peak negative pressure and  $F_c$  is the center frequency of the ultrasound wave. The MI is designed to assess the risk for cavitation phenomena, a process where ultrasound causes gas bubbles to form and expand in tissue. These bubbles implode when they reach a threshold size, with sufficient force to perforate cell membranes.

It has been argued that fetal tissue contains insufficient gas in solution for cavitation phenomena to occur. The MI has not been evaluated as a marker for non-cavitation mechanical effects, such as streaming.

Despite their limits, the MI and TI are valuable tools in monitoring fetal exposure to ultrasound and the risk for bioeffects. We recommend that one employs the lowest power setting that is compatible with obtaining the necessary clinical information. The guidelines of BMUS indicate no upper time limit for ultrasound examinations where the TIB is kept below 0.7 and the MI is kept below 0.3. TI above 3.0 and/or MI above 1.7 is not compatible with safe obstetric ultrasound. Doppler is not recommended as a routine modality in the first trimester, but can be used with caution for precision diagnostics where pathology is suspected [10].

---

## 7.6 What Can the Operator Do?

We recommend that ultrasound exposure be kept to the lowest level compatible with obtaining good-quality clinically relevant information. Studies indicate that such information can be obtained using intensities well below that which we have reason to believe is currently applied in most clinical settings [11, 12]. It seems that ultrasound scanners in clinical use are commonly used with the power set to 100%, and rarely reduced. There is also evidence pointing to insufficient knowledge of how to adjust output power

even among experienced operators of obstetric ultrasound [13].

We have compared Doppler examinations at different intensities of five clinically relevant vessels; the umbilical artery, fetal middle cerebral artery, ductus venosus, and both maternal uterine arteries. The examinations were done at TIB 1.0, 0.5, and 0.1, respectively. Relevant information was obtained in all cases; statistical analysis revealed no significant differences between measurements obtained at low and high intensities [11, 12] (Fig. 7.2).

Based on this, we recommend that the default power setting is set to 85% of the maximal value; normally, this would result in TIB below 0.7 and MI below 0.3. From this level, the examiner may increase the power when particularly difficult conditions necessitate this.

## 7.7 Evidence from Human Studies

For interpretation of data derived from epidemiological studies, there is a hierarchy of studies based on study design and the quality of the research methods. Highest value should be given to systematic reviews of randomized controlled trials, and less value to cohort studies, case-control studies, and other observational studies (in that order).

One randomized controlled trial has assessed the effect of regular Doppler ultrasound in low-risk pregnancies, reporting data on 1415 women who had frequent Doppler ultrasound throughout pregnancy and 1419 who did not. The aims of the trial were not to study safety aspects of Doppler ultrasound, but the results indicated increased risk for birth weight below the third centile (odds

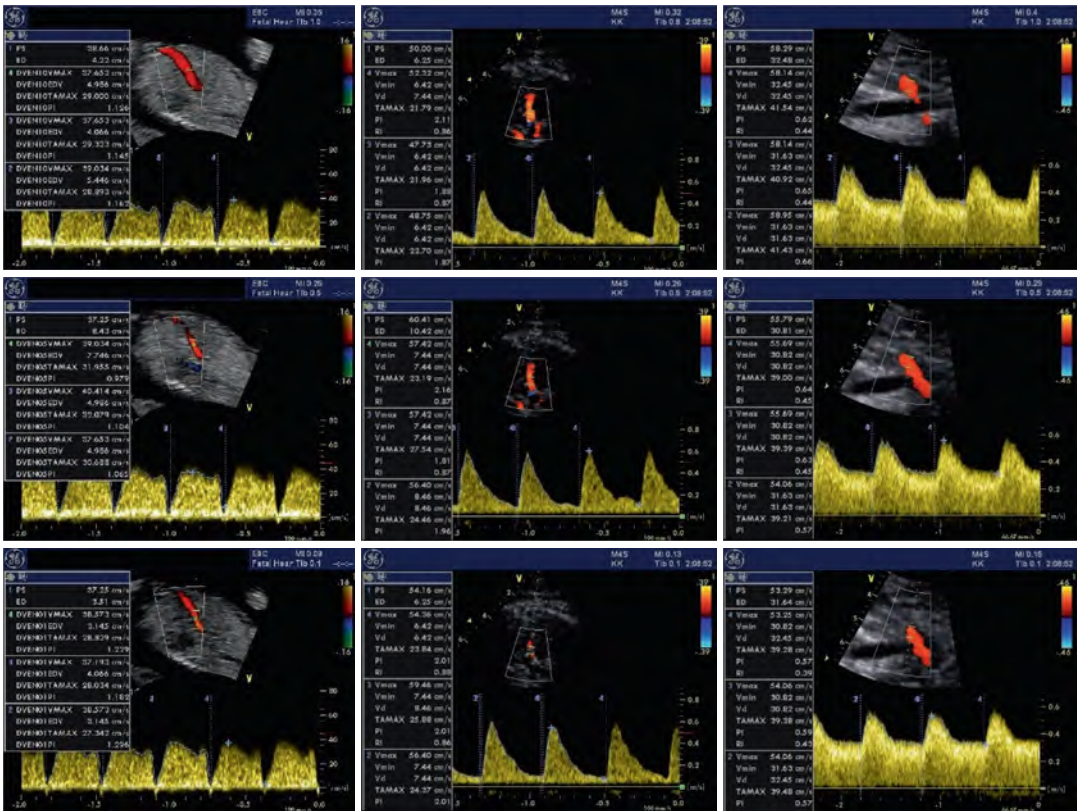


**Fig. 7.2** From left to right: Ductus venosus at 12 weeks, the middle cerebral artery at 18 weeks, and the right uterine artery at 24 weeks. Top row obtained at TIB 1.0, middle row at TIB 0.5, and bottom row at TIB 0.1

ratio 1.84) and below the tenth centile (odds ratio 1.46) [14].

A follow-up study was published 19 years after the initial trial. This study assessed development of autism spectrum disorders (ASD) [15]. There was no difference in the occurrence of ASD between the exposed group (7 cases of ASD among 1167 children) and the control group (9 cases of ASD among 1125 children) [15]. A subgroup of 586 cases and 595 controls was subject to assessment by a ASD quotient scale, and this analysis did not reveal any difference between the groups.

There are very few other epidemiological studies concerned with safety aspects of Doppler ultrasound. However, pulsed Doppler has the highest risk of producing adverse effects, and acoustic outputs from modern devices have increased 10–15-fold during the last decades. In addition, the number of scans per pregnancy and exposure times have increased over time. If there is evidence of adverse effects using lower acoustic outputs and exposure times, the users of the new generations of ultrasound scanners must acknowledge that there is a potential risk. Thus, there is a need to explore other available epidemiological evidence.

Two systematic reviews of epidemiological studies of the safety of ultrasound in pregnancy have been published [16, 17]. A Cochrane review [16] included all registered published and ongoing randomized controlled trials and quasi-randomized trials, but no other studies. An ISUOG-WHO review [17] included 16 controlled randomized controlled trials, 13 cohort, and 12 case-control studies published between January 1950 and October 2007 that assessed any type of short- and long-term effects of at least one expo-

sure to ultrasound during pregnancy. The outcomes assessed included maternal outcomes, perinatal outcomes, childhood growth, neurological development and school performance, non-right-handedness, childhood malignancies, intellectual performance, and mental diseases after childhood [17].

The conclusions from the systematic reviews are that epidemiological studies have demonstrated no confirmed associations between prenatal ultrasound and adverse perinatal outcomes, childhood malignancies, neurological development, dyslexia, speech development, school performance, intellectual performance, and adult mental disease. However, there is a weak statistically significant association between prenatal ultrasound and being non-right-handed.

According to the data presented in the Cochrane review [17], there was no statistically significant association between prenatal ultrasound and non-right-handedness. However, in a more recent meta-analysis including three randomized controlled trials, there was a statistically significant association [18] (Fig. 7.3).

If results from cohort studies are included [22, 23], as was done in the ISUOG-WHO review, the strength of the association was similar for randomized trials and cohort studies [17]. Thus, the conclusion must be that five epidemiological studies report a 15% increase in the likelihood of sinistrality (in particular among males), and no other epidemiological evidence contradicts this association.

The discussion of prenatal ultrasound and handedness is complex and will not be extended here. An editorial explores this issue in detail [24]. A statistical association between ultrasound and left-handedness should not lead to the con-

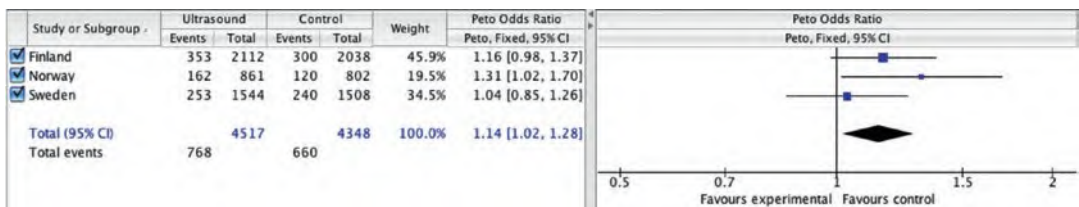


**Fig. 7.3** Forest plot of odds ratios of non-right-handedness according to randomized groups in a Finnish study [19], Norwegian study [20], Swedish study [21], and overall

clusion that ultrasound causes harm to the developing brain. The current biological understanding of handedness is limited and partly contradictory to the epidemiological evidence.

Autism spectrum disorder (ASD) is a neurodevelopmental disorder with mainly genetic origin, but there is evidence that environmental factors may play a role, and that the initiating process leading to ASD originates during fetal life. Reported registered prevalence rates are increasing, but it seems that much of the increase reflects better awareness of the disorder rather than a true rise in prevalence. Nevertheless, a recent study has created some concern.

Webb reported a case series of 1749 children with ASD aged 4–18 years. ASD severity was characterized using measures of cognitive ability, social ability, and repetitive behaviors [25]. Genetic predisposition was characterized by the presence of ASD-associated copy-number variations (CNV). The authors compared 84 exposed and 41 nonexposed children with ASD and CNV, and a subsample of 73 exposed and 38 nonexposed boys with ASD and CNV. They concluded that the combination of first trimester ultrasound and presence of CNV in male children with ASD correlated with poorer cognitive outcomes and increased repetitive behaviors. This study has a high risk of bias: it was a case-series with no control group, exposure information was collected by recall 4–18 years after the pregnancy, multiple testing without correction of statistical significance level was undertaken, and possible confounding factors were not addressed.

Three other studies of a possible association between ultrasound exposure and ASD have been published; one case-control study [26] and two long-term follow-up of a large number of children from randomized controlled trials [15, 27]. None of these studies found any association between prenatal ultrasound and ASD. Based on the available data, we must conclude that there is no scientifically proven association between ultrasound exposure in first or second trimester and ASD, or its severity.

## 7.8 Guidelines and Recommendations

Sonograms can be safely performed during pregnancy by trained and accredited sonologists, when medically indicated and when the “as low as reasonably achievable” (ALARA) principle on the use of ultrasound intensities is employed. Since, in Doppler mode, relatively high intensities are usually transmitted, ISUOG (and other ultrasound organizations) recommend that pulsed Doppler (spectral, power, and color flow imaging) ultrasound should not be used routinely in early pregnancy [10]. When performing Doppler ultrasound in the first trimester on clinical grounds, the displayed thermal index (TI) should be  $\leq 1.0$  and exposure time should be kept as short as possible.

## References

1. Duck FA, Martin K. Trends in diagnostic ultrasound exposure. *Phys Med Biol*. 1991;36:1423–32.
2. Henderson J, Wilson K, Jago J, Whittingham TA. A survey of the acoustic outputs of diagnostic ultrasound equipment in current clinical use in the Northern region. *Ultrasound Med Biol*. 1995;21:699–705.
3. Whittingham TA. The acoustic output of diagnostic machines. In: ter Haar G, Duck FA, editors. *The safe use of ultrasound in medical diagnosis*. 2nd ed. London: BMUS/BIR; 2000.
4. Martin K. The acoustic safety of new ultrasound technologies. *Ultrasound*. 2010;18:110–8. <https://doi.org/10.1258/ult.2010.010024>.
5. Nyborg WLCP, Carstensen EL, Dunn F, Miller D, Miller MW, Thompson HE, Ziskin MC. Exposure criteria for medical diagnostic ultrasound: II. Criteria based on all known mechanisms. National Council on Radiation Protection and Measurements 2002; Report NO 140.
6. Abramowicz JS, Kossoff G, Marsal K, Ter Haar G. Safety Statement, 2000 (reconfirmed 2003). International Society of Ultrasound in Obstetrics and Gynecology (ISUOG). *Ultrasound Obstet Gynecol*. 2003;21:100.
7. BMUS. Guidelines for the safe use of diagnostic ultrasound equipment. In: *The Safety Group of the British Medical Ultrasound Society, editor. Guidelines for the safe use of diagnostic ultrasound equipment*; 2009.
8. Bigelow TA, Church CC, Sandstrom K, Abbott JG, Ziskin MC, Edmonds PD, Herman B, Thomenius KE, Teo TJ. The thermal index: its strengths, weaknesses, and proposed improvements. *J Ultrasound Med*. 2011;30:714–34.